frontiers in Energy Research

ORIGINAL RESEARCH
published: 17 March 2021
doi: 10.3389/fenrg.2021.640777

Room-Temperature Mg-Ion Conduction Through Molecular Crystal $Mg\{N(SO_2CF_3)_2\}_2(CH_3OC_5H_9)_2$

Takaaki Ota[1], *Shota Uchiyama*[1], *Keiichi Tsukada*[1] *and Makoto Moriya*[1,2]*

[1]Department of Science, Graduate School of Integrated Science and Technology, Shizuoka University, Shizuoka, Japan, [2]College of Science, Academic Institute, Shizuoka University, Shizuoka, Japan

Molecular crystals have attracted increasing attention as a candidate for innovative solid electrolytes with solid-state Mg-ion conductivity. In this work, we synthesized a novel Mg-ion-conducting molecular crystal, $Mg\{N(SO_2CF_3)_2\}_2(CH_3OC_5H_9)_2$ ($Mg(TFSA)_2(CPME)_2$), composed of Mg bis(trifluoromethanesulfonyl)amide ($Mg(TFSA)_2$) and cyclopentyl methyl ether (CPME) and elucidated its crystal structure. We found that the obtained $Mg(TFSA)_2(CPME)_2$ exhibits solid-state ionic conductivity at room temperature and a high Mg-ion transference number of 0.74. Contrastingly, most Mg-conductive inorganic solid electrolytes require heating above 150–300°C to exhibit ionic conductivity. These results further prove the suitability of molecular crystals as candidates for Mg-ion-conducting solid electrolytes.

Keywords: magnesium, solid electrolyte, ion conduction, molecular crystal, battery

OPEN ACCESS

Edited by:
Jun Mei,
Queensland University of Technology, Australia

Reviewed by:
Qian Zhang,
Taiyuan University of Technology, China
Liaoyun Zhang,
University of Chinese Academy of Sciences, China
Michael Horn,
Queensland University of Technology, Australia

***Correspondence:**
Makoto Moriya
moriya.makoto@shizuoka.ac.jp

Specialty section:
This article was submitted to Electrochemical Energy Conversion and Storage, a section of the journal Frontiers in Energy Research

Received: *12 December 2020*
Accepted: *27 January 2021*
Published: *17 March 2021*

Citation:
Ota T, Uchiyama S, Tsukada K and Moriya M (2021) Room-Temperature Mg-Ion Conduction Through Molecular Crystal $Mg\{N(SO_2CF_3)_2\}_2(CH_3OC_5H_9)_2$. Front. Energy Res. 9:640777. doi: 10.3389/fenrg.2021.640777

INTRODUCTION

Rechargeable Mg batteries are a promising candidate for high-energy-density, low-cost storage batteries, owing to their high negative reduction potential (NHE vs. −2.356 V) and large capacity (3,832 mA h cm^{-3}) as anodes, as well as the abundance of Mg in the Earth's crust (Aurbach et al., 2000; Besenhard and Winter, 2002; Aurbach et al., 2007; Muldoon et al., 2012; Yoo et al., 2013; Mohtadi and Mizuno, 2014). Moreover, it is critical to expedite the development of Mg-ion conductive solid electrolytes for the realization of all-solid-state Mg batteries (Deivanayagam et al., 2019). This can address the leakage and combustion of liquid electrolytes, which is a grave limitation of lithium-ion batteries. For decades, the development of solid electrolytes with Mg-ion conductivity based on ceramics and glass has been the subject of extensive research (Ikeda et al., 1987; Imanaka et al., 2000; Imanaka et al., 2001; Kawamura et al., 2001; Higashi et al., 2014; Yamanaka et al., 2014; Adamu and Kale 2016). It has been reported that the Mg-ions in these inorganic solid electrolytes diffuse through the conduction paths in these materials. However, most of the reported inorganic electrolytes require temperatures exceeding 150°C to exhibit Mg-ion conductivity. Recently, a room-temperature ionic conductivity of 0.1 mS cm^{-1} for $MgSc_2Se_4$ has been reported; however, its high electronic conductivity (0.04% of ionic conductivity) hampers the application as an electrolyte (Canepa et al., 2017). Hence, innovative electrolyte materials that enable fast and selective Mg-ion conduction at room temperature are crucial for realizing practical Mg batteries.

Molecular crystals have attracted considerable attention as candidates for solid electrolytes. These molecular crystalline electrolytes comprise organic molecules and metal salts and possess ion conduction paths in the crystal lattice; the paths are organized by molecular arrangement (Moriya et al., 2012; Moriya et al., 2013; Moriya et al., 2014; Moriya et al., 2016; Moriya, 2017;

Tanaka et al., 2020). The structure of the ion conduction paths is precisely controlled to improve conductivity by modifying the type of organic molecules or metal salts employed as the building blocks. We previously discovered that the molecular crystal Li$\{N(SO_2F)_2\}(NCCH_2CH_2CN)_2$ exhibits a high Li-ion conductivity of 10^{-4} S cm^{-1} at room temperature, and reported the fabrication of an all-solid-state battery using Li$\{N(SO_2F)_2\}(NCCH_2CH_2CN)_2$ as a solid electrolyte via a simple process based on the melting and solidification of this electrolyte (Tanaka et al., 2020).

Recently, an ionic conductivity of 5×10^{-8} S cm^{-1} (30°C) was reported for a molecular crystal depicted as $Mg(BH_4)_2(H_2NCH_2CH_2NH_2)$ that comprised $Mg(BH_4)_2$ and ethylenediamine. However, the crystal structure of $Mg(BH_4)_2(H_2NCH_2CH_2NH_2)$ was not elucidated and the Mg-ion transference number was not evaluated (Roedern et al., 2017).

Therefore, we investigated the development of novel molecular crystalline electrolytes consisting of MgTFSA and an organic molecule, based on our previous work on molecular crystalline electrolytes. Herein, we report the synthesis of a molecular crystal, $Mg\{N(SO_2CF_3)_2\}_2(CH_3OC_5H_9)_2$ ($Mg(TFSA)_2(CPME)_2$) with room temperature Mg-ion conductivity resulting from the reaction of magnesium bis(trifluoromethanesulfonyl)amide ($Mg(TFSA)_2$) and cyclopentyl methyl ether (CPME). We also discuss the results of single-crystal X-ray structure analysis, the evaluation of the ionic conductivity, and the Mg-ion transference number for $Mg(TFSA)_2(CPME)_2$.

MATERIALS AND METHODS

General

All experiments were carried out under an Ar atmosphere using Schlenk techniques or in an Ar-filled glovebox (MBraun, UNIlab2000). CPME (dehydrated) was purchased from FUJIFILM Wako Pure Chemical Industry Corporation. Mg$\{N(SO_2CF_3)_2\}_2$ ($Mg(TFSA)_2$) was purchased from Kishida Chemical Co., Ltd. The CPME was used as purchased, without any modifications. Furthermore, $Mg(TFSA)_2$ was dried under reduced pressure at 50°C for 3 days prior to use.

Synthesis of $Mg(TFSA)_2(CPME)_2$

$Mg(TFSA)_2$ (1.005 g, 1.72 mmol) and CPME (0.400 mL, 3.44 mmol) were charged into a 50 mL Schlenk tube and heated until the mixture melted. Subsequently, the reaction flask was cooled to room temperature and stored for 4 days at −30°C to quantitatively obtain $Mg(TFSA)_2(CPME)_2$ in the form of colorless single crystals. Although the crystals were highly deliquescent and immediately absorbed water from the air to form a highly viscous liquid, they could be handled stably at room temperature in an Ar atmosphere.

Characterization of $Mg(TFSA)_2(CPME)_2$

Differential scanning calorimetry (DSC) was performed on a Shimadzu DSC60 instrument operated at a heating rate of 10°C min^{-1} under a N_2 atmosphere, using Al_2O_3 as the reference material. Infrared (IR) spectra were recorded on a Shimadzu IRSpirit using pellet samples with $Mg(TFSA)_2(CPME)_2$ diluted in KBr. Powder X-ray diffraction (XRD) was measured at room temperature on a Rigaku SmartLab diffractometer, using Cu-K_α radiation with a monochromator. The powder sample for XRD was prepared by grinding the crystals of $Mg(TFSA)_2(CPME)_2$ in a glovebox. For measurement, the powder sample was placed on a non-reflective silicon plate and covered with Kapton film and tape to prevent the samples from absorbing moisture.

Single-crystal X-ray diffraction to reveal the crystal structure was performed using the Rigaku VariMax Saturn system (Mo-$K\alpha$ radiation, 1.2 kW rotating anode). The crystal data for $C_{16}H_{24}F_{12}MgN_2O_{10}S_4$ (MW: 784.90) are given as follows: tetragonal, Space Group P-1 (no. 2), a = 9.474(2) Å, b = 9.671(2) Å, c = 17.137(4) Å, α = 99.193(3) °, β = 93.438(4) °, γ = 104.684(3) °, V = 1,491.0(6) Å, Z = 2, T = −150.0°C, μ(MoKα) = 4.656 cm^{-1}, D_{calc} = 1.748 g/cm^3, reflections collected/unique reflections/parameters refined: 23905/6831/424, R_{int} = 0.0440, final R_1 = 0.0560 ($I > 2\sigma(I)$), wR_2 = 0.1675 (all data), and GOF = 1.114.

The Cambridge Crystallographic Data Centre (CCDC) 2049209 contains the supplementary crystallographic data for $Mg(TFSA)_2(CPME)_2$. The data can be obtained free of charge via http://www.ccdc.cam.ac.uk/conts/retrieving.html (or from the CCDC, 12 Union Road, Cambridge CB2 1EZ, United Kingdom; Fax: +44 1223 336033; E-mail: deposit@ccdc.cam.ac.uk).

The ionic conductivity of the sample was measured via the AC impedance method using Biologic, VMP3, in the frequency range of 1 Hz to 1 MHz and the temperature range of 10–40°C. The powder samples of $Mg(TFSA)_2(CPME)_2$ were pressed into disks in a glovebox and placed between two SUS plates in a closed vessel with a two-electrode cell. The temperature of the samples was controlled in a bench-top-type chamber (Espec, SU-241), and all the cells were equilibrated at the operating temperature for 3 h before commencing measurements. The AC impedance data displayed either a well-defined semicircle and a low-frequency spike, or only a low-frequency spike. The ionic conductivity (σ) was calculated using $\sigma = l/SR$, where R is the bulk resistance (Ω), S is the area (cm^2) of the Au electrodes, and l is the thickness of the electrolyte material (cm). The bulk resistance was calculated from the touchdown point of the electrolyte on the Re|Z|-axis in a Nyquist plot.

The magnesium transference number (t_{Mg2+}) for $Mg(TFSA)_2(SN)_2$ was measured using a symmetric cell with Mg electrodes, Mg|$Mg(TFSA)_2(CPME)_2$|Mg, at 40°C. The method developed by Vincent et al. was used to calculate the transference number, as follows (Evans et al., 1987):

$$t_{Mg2+} = I_s(\Delta V - I_0R_0)/I_0(\Delta V - I_sR_s),$$

where R_0 is the initial resistance, I_0 denotes the initial current, R_s represents the steady-state resistance, and I_s is the steady-state current.

R_0 and I_0 were estimated by means of AC impedance measurements, and a DC polarization measurement (ΔV = 1.0 V) was carried out on the cell after equilibrating the cell at 40°C for 120 h. The current was obtained as a function of time, and I_s was measured; R_s was estimated by means of AC impedance measurements. In this measurement, I_0 and I_s were

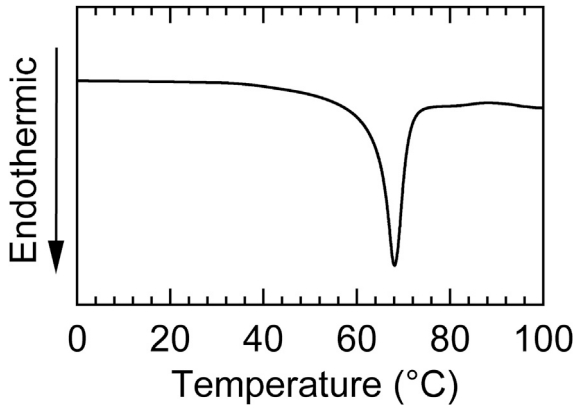

FIGURE 1 | Differential scanning calorimetry (DSC) curves of $Mg(TFSA)_2(CPME)_2$ under N_2 flow.

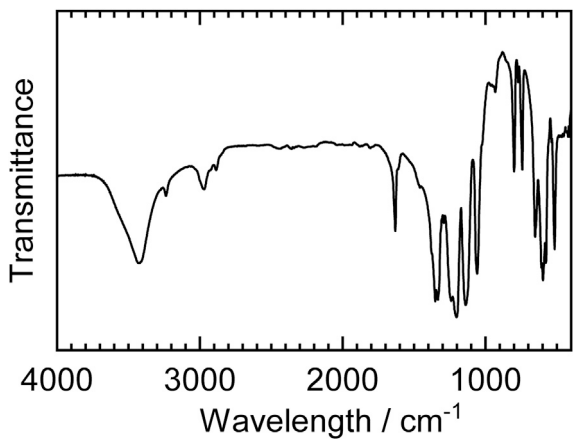

FIGURE 2 | IR spectrum of $Mg(TFSA)_2(CPME)_2$.

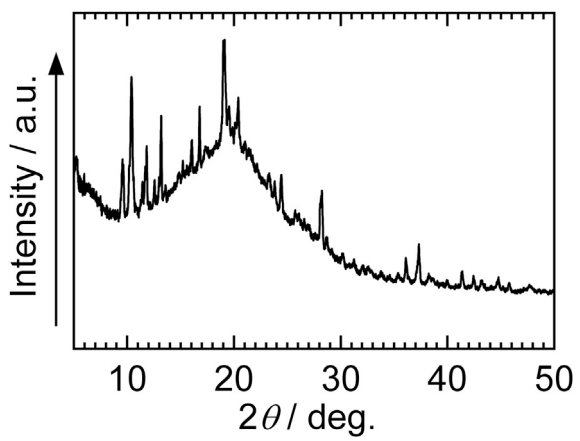

FIGURE 3 | Powder XRD pattern of $Mg(TFSA)_2(CPME)_2$. (The broad peak observed in the range of 15°–25° is derived from the Kapton film employed to prevent $Mg(TFSA)_2(CPME)_2$ from absorbing moisture.).

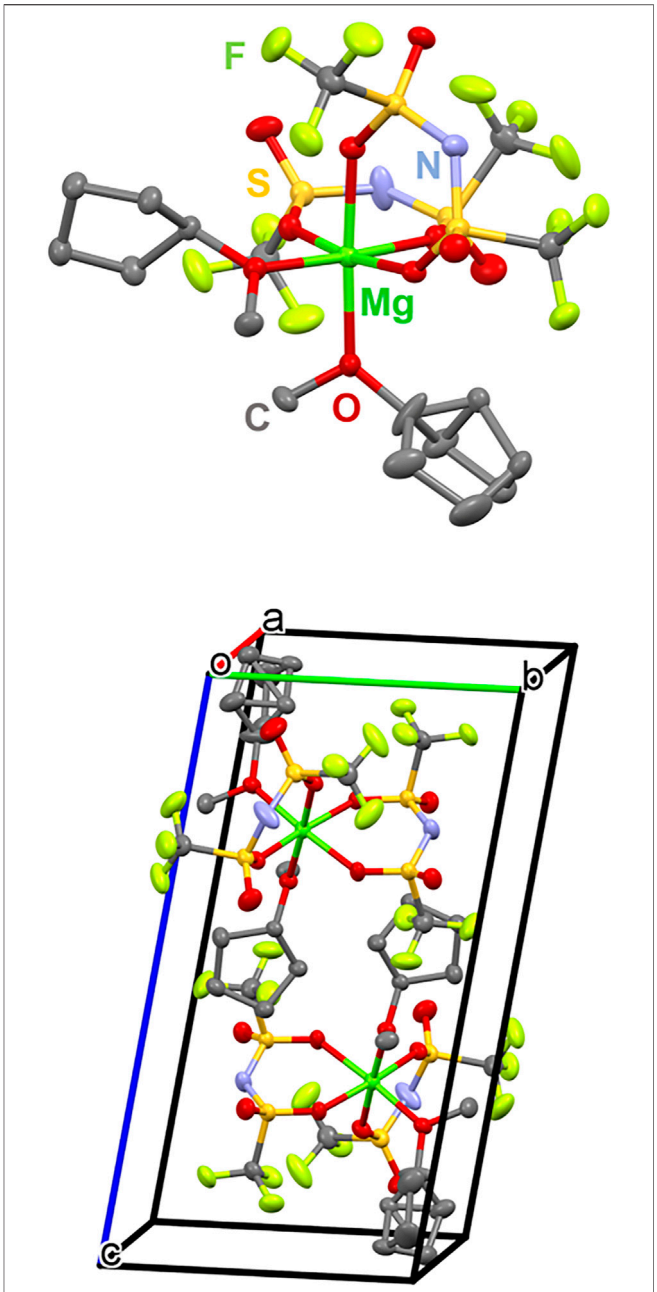

FIGURE 4 | Crystal structure **(top)** and unit cell structure **(bottom)** of $Mg(TFSA)_2(CPME)_2$ with thermal ellipsoids at the 40% probability level (Mg: green, C: gray, N: pale blue, O: red, F: pale green, and S: dark yellow. H atoms are omitted for clarity).

estimated to be 2.85 and 2.12 μA, respectively. R_0 and R_s were evaluated to be 10,085 and 10,227 Ω, respectively.

RESULTS AND DISCUSSION

$Mg(TFSA)_2(CPME)_2$ was obtained in the form of colorless columnar crystals by heating $Mg(TFSA)_2$ with 2.0 M amounts

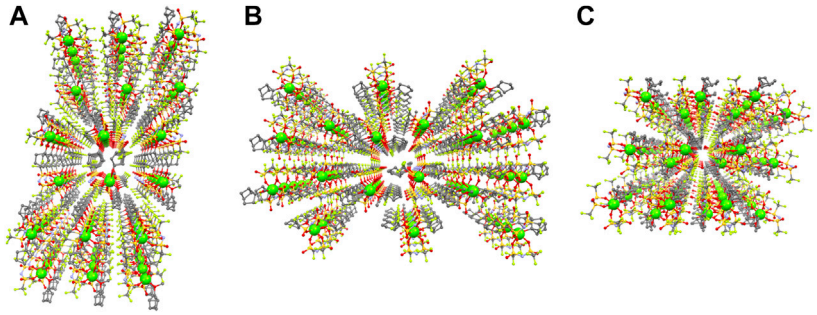

FIGURE 5 | Packing view with ball and stick model of $Mg(TFSA)_2(CPME)_2$. Mg-ions are emphasized as a large sphere. **(A)** along the *a*-axis **(B)** along the *b*-axis, and **(C)** along the *c*-axis (Mg: green, **C**: gray, N: pale blue, O: red, **F**: pale green, and S: dark yellow. H atoms are omitted for clarity).

of CPME, followed by cooling the resulting melt to room temperature. From the DSC curve (**Figure 1**), the melting point of $Mg(TFSA)_2(CPME)_2$ was estimated to be 66°C. We confirmed that the DSC curve of the sample prepared by cooling the melt of $Mg(TFSA)_2(CPME)_2$ results in an endothermic peak at an identical temperature to that of the DSC curve in **Figure 1**. The results show that the structural change of $Mg(TFSA)_2(CPME)_2$ during melting and solidification is reversible. The IR spectrum of $Mg(TFSA)_2(CPME)_2$ is exhibited in **Figure 2**. In this result, absorptions attributable to S=O and C–F bonds in the TFSA moiety and C-O bonds in the CPME units are observed in the region from 1,000 to 1,500 cm^{-1}, similar to the IR spectra of the previously reported $Mg(TFSA)_2$-based electrolyte containing diglyme (Ha et al., 2014). The powder XRD pattern of the $Mg(TFSA)_2(CPME)_2$ gave sharp diffractions to show that the compound has high crystallinity (**Figure 3**).

The crystal structure of $Mg(TFSA)_2(CPME)_2$ was revealed by a single-crystal XRD study, as shown in **Figure 4**. It is evident that $Mg(TFSA)_2(CPME)_2$ is formed as a mononuclear Mg complex with a hexa-coordinated octahedral structure. Two molecules of CPME were coordinated to the Mg-ion via the O atom of the ether group. These CPME molecules were located in the cis position to the Mg center, and the cyclopentyl groups in the CPME molecules were located toward the opposite position to avoid steric repulsion. One of the CPME molecules possessed disorder in the cyclopentyl group. The remaining four coordination sites on Mg were occupied by the chelation of two TFSA anions via the O atom of a sulfonyl group.

Figure 5 shows the packing diagrams of $Mg(TFSA)_2(CPME)_2$ along the *a*-, *b*-, and *c*-axes. Ordered arrangements of Mg-ions were recognized in each direction, corresponding to the ion conduction paths. From the packing view, the nearest intermolecular Mg–Mg distance was estimated to be 8.769 Å. Notably, the previously reported LiTFSA-based molecular crystalline electrolytes with similar nearest Li–Li distances were found to exhibit selective Li-ion conductivity at room temperature ((Moriya et al., 2012; Moriya et al., 2013; Moriya et al., 2014; Moriya et al., 2016). These results suggest that $Mg(TFSA)_2(CPME)_2$ also shows room-temperature Mg-ion conductivity.

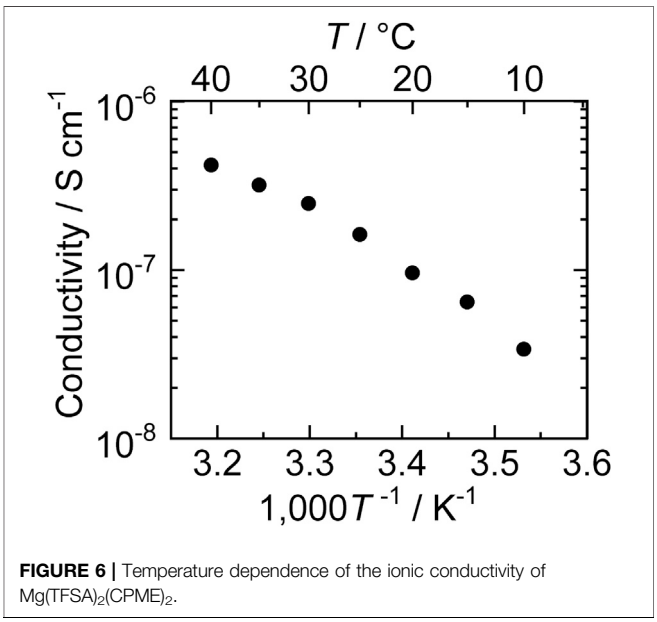

FIGURE 6 | Temperature dependence of the ionic conductivity of $Mg(TFSA)_2(CPME)_2$.

The ionic conductivity of $Mg(TFSA)_2(CPME)_2$ in the crystalline state was evaluated using AC impedance measurements, and the solid-state ionic conductivities were observed from 10 to 40°C. The powder sample that was obtained by milling the $Mg(TFSA)_2(CPME)_2$ single crystals, pressed into a disk, and sandwiched between two Au electrodes was employed for the measurements. From the measurements, we found that $Mg(TFSA)_2(CPME)_2$ exhibited 2.5 times higher ionic conductivity at around room temperature than the previously reported molecular crystal $Mg(BH_4)_2(H_2NCH_2CH_2NH_2)$. An ionic conductivity of 2×10^{-7} S cm^{-1} at 30°C was noted for $Mg(TFSA)_2(CPME)_2$, while that of $Mg(BH_4)_2(H_2NCH_2CH_2NH_2)$ was 8×10^{-8} S cm^{-1} at 30°C (**Figure 6**) (Roedern et al., 2017).

The Arrhenius plot of $Mg(TFSA)_2(CPME)_2$ exhibits linearity, similar to the lithium ion-conducting molecular crystalline electrolytes previously reported by our group. Based on this result, the activation energy for ion conduction through $Mg(TFSA)_2(CPME)_2$ was calculated to be 69 kJ mol^{-1}.

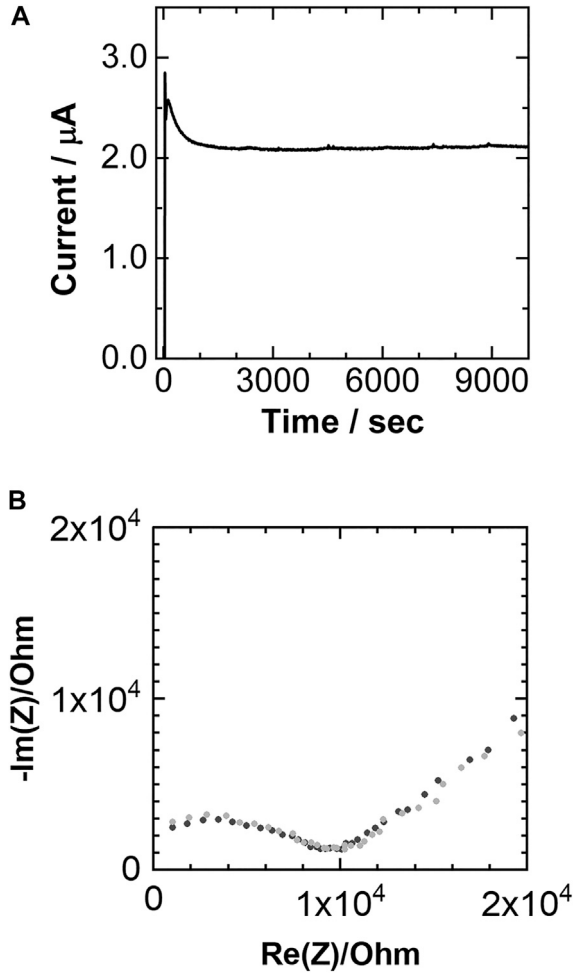

FIGURE 7 | (A) Time dependence of current with DC polarization voltage of 1.0 V for Mg|Mg(TFSA)$_2$(CPME)$_2$|Mg at 40°C for estimating the Mg-ion transference number; **(B)** Nyquist plots of Mg|Mg(TFSA)$_2$(CPME)$_2$|Mg at 40°C; (black) taken before the DC polarization measurement (gray) taken after the current of the DC polarization reaches steady state.

Interestingly, this activation energy was comparable to the previously reported values for lithium ion-conductive molecular crystals, such as Li(TFSA)(1,2-dimethoxybenzene) (78 kJ mol^{-1}) and Li(TFSA)(1,2-dimethoxybenzene)$_2$ (84 kJ mol^{-1}). Furthermore, the linearity of the Arrhenius plot suggests that the ionic conduction is induced by a hopping mechanism in the crystal lattice similar to the LiTFSA-based molecular crystals.

The Mg-ion transference number (t_{Mg2+}) for Mg(TFSA)$_2$(CPME)$_2$ was measured using Mg metal electrodes, following a previously reported method (Evans et al., 1987). The DC polarization and AC impedance measurements on the cell Mg | Mg(TFSA)$_2$(CPME)$_2$ | Mg are shown in **Figure 7**. Based on these results, the value of the t_{Mg2+} was estimated to be 0.74. The t_{Mg2+} value of Mg(TFSA)$_2$(CPME)$_2$ is considerably higher than the reported value of polymer-based Mg-ion conductive electrolytes. For example, the t_{Mg2+} of polyethylene oxide (PEO) containing Mg(CF$_3$SO$_3$)$_2$ salt and 1-ethyl-3-methylimidazolium tetrafluoroborate ionic liquid has been reported to be 0.22 (Maheshwaran et al., 2020). The high t_{Mg2+} value and linearity of the Arrhenius plots obtained during conductivity measurements strongly suggest that Mg-ion conduction preferentially takes place via a hopping mechanism in the crystal lattices of Mg(TFSA)$_2$(CPME)$_2$.

CONCLUSION

In this study, we successfully developed a novel molecular crystalline electrolyte, Mg(TFSA)$_2$(CPME)$_2$, with Mg-ion conductivity at room temperature using Mg(TFSA)$_2$ salt and CPME. Single-crystal X-ray structure analysis revealed that the molecular crystal Mg(TFSA)$_2$(CPME)$_2$ displays ordered arrangements of Mg-ions in the crystal lattice, corresponding to the ionic conduction paths. We confirmed that the fabricated electrolyte exhibits a room-temperature ionic conductivity of 10^{-7} S cm^{-1} and a high Mg-ion transference number of 0.74 in the crystalline state through electrochemical measurements. These results demonstrate the considerable potential of molecular crystals for application as solid electrolytes in rechargeable Mg batteries.

DATA AVAILABILITY STATEMENT

The datasets presented in this study can be found in online repositories. The names of the repository/repositories and accession number(s) can be found below: CCDC 2049209 contains the supplementary crystallographic data for this paper. These data can be obtained free of charge via http://www.ccdc.cam.ac.uk/conts/retrieving.html.

AUTHOR CONTRIBUTIONS

TO, SU, and MM designed the experiments and wrote the paper. TO and SU synthesized the electrolyte and evaluated the thermal behavior and Mg-ion conductive properties. KT performed IR and XRD measurements. MM performed the crystal structural analysis.

FUNDING

MM acknowledges the funding provided by JSPS Kakenhi (Grant Nos. JP17K14460 and JP20K21079), Nippon Sheet Glass Foundation for Materials and Engineering, and JST A-STEP (JPMJTR20TH).

REFERENCES

Adamu, M., and Kale, G. M. (2016). Novel sol-Gel synthesis of MgZr4P6O24 composite solid electrolyte and newer insight into the Mg2+-ion conducting properties using impedance spectroscopy. *J. Phys. Chem. C* 120, 17909–17915. doi:10.1021/acs.jpcc.6b05036

Allred, H. D., Shterenberg, I., Gofer, Y., Gershinsky, G., Pour, N., and Aurbach, D. (2013). Mg rechargeable batteries: an on-going challenge. *Energy Environ. Sci.* 6, 2265–2279. doi:10.1039/c3ee40871j

Aurbach, D., Lu, Z., Schechter, A., Gofer, Y., Gizbar, H., Turgeman, R., et al. (2000). Prototype systems for rechargeable magnesium batteries. *Nature* 407, 724–727. doi:10.1038/35037553

Aurbach, D., Suresh, G. S., Levi, E., Mitelman, A., Mizrahi, O., Chusid, O., et al. (2007). Progress in rechargeable magnesium battery technology. *Adv. Mater.* 19, 4260–4267. doi:10.1002/adma.200701495

Muldoon, J., Bucur, C. B., Oliver, A. G., Sugimoto, T., Matsui, M., Kim, H. S., et al. (2012). Electrolyte roadblocks to a magnesium rechargeable battery. *Energ. Environ. Sci.* 5, 5941–5950. doi:10.1039/c2ee03029b

Canepa, P., Bo, S.-H., Sai Gautam, G., Key, B., Richards, W. D., Shi, T., et al. (2017). High magnesium mobility in ternary spinel chalcogenides. *Nat. Commun.* 8, 1759. doi:10.1038/s41467-017-01772-1

Besenhard, J. O., and Winter, M. (2002). Advances in battery technology: rechargeable magnesium batteries and novel negative-electrode materials for lithium ion batteries. *Chemphyschem* 3, 155–159. doi:10.1002/1439-7641(20020215)3:2<155::aid-cphc155>3.0.co;2-s

Deivanayagam, R., Ingram, B. J., and Shahbazian-Yassar, R. (2019). Progress in development of electrolytes for magnesium batteries. *Energ. Storage Mater.* 21, 136–153. doi:10.1016/j.ensm.2019.05.028

Evans, J., Vincent, C. A., and Bruce, P. G. (1987). Electrochemical measurement of transference numbers in polymer electrolytes. *Polymer* 28, 2324–2328. doi:10.1016/0032-3861(87)90394-6

Ha, S.-Y., Lee, Y.-W., Woo, S. W., Koo, B., Kim, J.-S., Cho, J., et al. (2014). Magnesium(II) bis(trifluoromethane sulfonyl) imide-based electrolytes with wide electrochemical windows for rechargeable magnesium batteries. *ACS Appl. Mater. Int.* 6, 4063–4073. doi:10.1021/am405619v

Ikeda, S., Takahashi, M., Ishikawa, J., and Ito, K. (1987). Solid electrolytes with multivalent cation conduction. 1. Conducting species in Mg·Zr·PO_4 system. *Solid State Ionics* 23, 125–129. doi:10.1016/0167-2738(87)90091-9

Imanaka, N., Okazaki, Y., and Adachi, G.-Y. (2000). Divalent magnesium ion conducting characteristics in phosphate based solid electrolyte composites. *J. Mater. Chem.* 10, 1431–1435. doi:10.1039/a909599c

Imanaka, N., Okazaki, Y., and Adachi, G. (2001). Optimization of divalent magnesium ion conduction in phosphate based polycrystalline solid electrolytes. *Ionics* 7, 440–446. doi:10.1007/bf02373581

Higashi, S., Miwa, K., Aoki, M., and Takechi, K. (2014). A novel inorganic solid state ion conductor for rechargeable Mg batteries. *Chem. Commun.* 50, 1320–1322. doi:10.1039/c3cc47097k

Kawamura, J., Morota, K., Kuwata, N., Nakamura, Y., Maekawa, H., Hattori, T., et al. (2001). High temperature 31P NMR study on Mg2+ ion conductors. *Solid State Commun.* 120, 295–298. doi:10.1016/s0038-1098(01)00386-6

Maheshwaran, C., Kanchan, D. K., Gohel, K., Mishra, K., and Kumar, D. (2020). Effect of Mg(CF3SO3)2 concentration on structural and electrochemical properties of ionic liquid incorporated polymer electrolyte membranes. *J. Solid State Electrochem.* 24, 655–665. doi:10.1007/s10008-020-04507-3

Mohtadi, R., and Mizuno, F. (2014). Magnesium batteries: current state of the art, issues and future perspectives. *Beilstein J. Nanotechnol.* 5, 1291–1311. doi:10.3762/bjnano.5.143

Roedern, E., Kühnel, R.-S., Remhof, A., and Battaglia, C. (2017). Magnesium ethylenediamine borohydride as solid-state electrolyte for magnesium batteries. *Sci. Rep.* 7, 46189. doi:10.1038/srep46189

Moriya, M. (2017). Construction of nanostructures for selective lithium ion conduction using self-assembled molecular arrays in supramolecular solids. *Sci. Technol. Adv. Mater.* 18, 634–643. doi:10.1080/14686996.2017.1366816

Moriya, M., Kato, D., Hayakawa, Y., Sakamoto, W., and Yogo, T. (2016). Crystal structure and solid state ionic conductivity of molecular crystal composed of lithium bis(trifluoromethanesulfonyl)amide and 1,2-dimethoxybenzene in a 1:1 molar ratio. *Solid State Ionics* 285, 29–32. doi:10.1016/j.ssi.2015.05.012

Moriya, M., Kato, D., Sakamoto, W., and Yogo, T. (2013). Structural design of ionic conduction paths in molecular crystals for selective and enhanced lithium ion conduction. *Chem. Eur. J.* 19, 13554–13560. doi:10.1002/chem.201300106

Moriya, M., Kitaguchi, H., Nishibori, E., Sawa, H., Sakamoto, W., and Yogo, T. (2012). Molecular ionics in supramolecular assemblies with channel structures containing lithium ions. *Chem. Eur. J.* 18, 15305–15309. doi:10.1002/chem.201202056

Moriya, M., Nomura, K., Sakamoto, W., and Yogo, T. (2014). Precisely controlled supramolecular ionic conduction paths and their structure-conductivity relationships for lithium ion transport. *CrystEngComm* 16, 10512–10518. doi:10.1039/c4ce01417k

Tanaka, K., Tago, Y., Kondo, M., Watanabe, Y., Nishio, K., Hitosugi, T., et al (2020). High Li-ion conductivity in Li{N(SO2F)2}(NCCH2CH2CN)2 molecular crystal. *Nano Lett.* 20, 8200–8204. doi:10.1021/acs.nanolett.0c03313

Yamanaka, T., Hayashi, A., Yamauchi, A., and Tatsumisago, M. (2014). Preparation of magnesium ion conducting MgS-P2S5-MgI2 glasses by a mechanochemical technique. *Solid State Ionics* 262, 601–603. doi:10.1016/j.ssi.2013.10.037

Conflict of Interest: The authors declare that the research was conducted in the absence of any commercial or financial relationships that could be construed as a potential conflict of interest.